Eur Biophys J (2006) 35: 373–381
DOI 10.1007/s00249-006-0044-z

ARTICLE

Manami Nishizawa · Kazuhisa Nishizawa

Interaction between K^+ channel gate modifier hanatoxin and lipid bilayer membranes analyzed by molecular dynamics simulation

Received: 9 November 2005 / Revised: 3 January 2006 / Accepted: 6 January 2006 / Published online: 2 February 2006

Abstract Hanatoxin (HaTx) is an ellipsoidal-shaped peptide that binds to the voltage sensor of voltage-dependent channels. Of physicochemical interest, HaTx has a "ring" of charged residues around its periphery and a hydrophobic protrusion. It has previously been postulated that HaTx binds to and functions on the surface of membranes, but a recent fluorescent-quenching study has implied a fairly deep positioning of HaTx in the lipid bilayer membrane. We carried out numerous molecular dynamic simulations of HaTx1, a well-studied variant of HaTx, in fully hydrated phospholipid bilayers. The system reproduced the surface-binding mode of HaTx1, in which HaTx1 resided in the extracellular side (outer) of the water/membrane interface with the hydrophobic patch of HaTx1 facing the membrane interior. On the other hand, analyses with various parameter settings suggested that the surface-binding mode was unstable because of the substantial attractive electrostatic force between HaTx1 and the lipid head groups of the inner (opposite) leaflet. Compared with this electrostatic force, the energetic cost for membrane deformation involving meniscus formation appeared to be small. In an attempt to interpret the quenching data, we consider the possibility of dimpling (meniscus formation) that brings HaTx1 inward (only ~0.7–0.8 nm above the bilayer center), while accounting for the flexibility of both leaflets of the membrane and the long-range interaction between positively charged residues of the membrane-bound peptide and the polar head groups of the opposite leaflet of the membrane. It is suggested that molecular dynamics simulations taking into account the flexibility of the membrane surface is potentially useful in interpreting the fluorescence-quenching data.

Keywords Molecular dynamics simulation · Lipid–protein interactions · Structural modelling

Electronic Supplementary Material Supplementary material is available for this article at http://dx.doi.org/10.1007/s00249-006-0044-z and is accessible for authorized users.

M. Nishizawa · K. Nishizawa (✉)
Department of Biochemistry, Teikyo University School of Medicine, Kaga, Itabashi, 173-8605 Tokyo, Japan
E-mail: kazunet@med.teikyo-u.ac.jp
Fax: +81-3-53756366

Introduction

Voltage-gated ion channels are a large family of membrane proteins playing a crucial role in regulating membrane potential and various cellular functions (Hille 2001). Voltage-activated K^+ (Kv) channels are tetrameric membrane proteins with each alpha subunit containing six (S1–S6) transmembrane segments. A primary function of the S1 through S4 segments in Kv channels is to sense voltage changes in the membrane.

A variety of peptide toxins isolated from the venom of spiders, scorpions and other organisms have drawn the attention of researchers because of their ability to inhibit voltage-gated ion channels (Ruta et al. 2003 and the references cited therein). Hanatoxin1 (HaTx1), isolated from Chilean tarantula (*Grammostola spatulata*) venom, is a 35 amino acid residue gating modifier of voltage-gated K^+ channels (Swartz and MacKinnon 1995, 1997; Li-Smerin and Swartz 1998). HaTx (a mixture of HaTx1 and HaTx2, which are identical except for residue 13 which is Ser in HaTx1 and Ala in HaTx2) can bind to closed channels (Lee et al. 2003), yet it exhibits very slow action ($\tau = 114$ s) despite its high affinity to the voltage sensor of the Kv2.1 channel (K_d = 42 nM) (Swartz and MacKinnon 1995). This and other findings suggest the involvement of some uncharacterized mechanisms governing the within-membrane dynamics of HaTx. HaTx is an ellipsoidal peptide that has a belt (or ring) of charged residues around its periphery and a hydrophobic patch (protrusion). How this unique structure supports the within-membrane dynamics and functions of HaTx is largely unknown.

Owing to many recent efforts, the treatment of lipid bilayer membranes in molecular dynamics simulations

has improved (e.g., Tieleman et al. 1997), allowing systems involving complex membrane proteins to be studied (reviewed in, e.g., Forrest and Sansom 2000; Hansson et al. 2002; Domene et al. 2003; Ash et al. 2004). Interactions between HaTx (and related toxins) and membranes, which is challenging to study experimentally, may also be suited for study by molecular dynamics simulations. Mutational analyses have led the authors to a rather naive postulation of the HaTx–membrane binding mode, in which the hydrophobic protrusion faces the hydrophobic interior of the bilayer membrane (Lee et al. 2003; Wang et al. 2004). However, a recent fluorescent-quenching study showed that the Trp30 of HaTx resides near the C9 or C10 atom of the acyl chains of the bilayer lipid (Phillips et al. 2005). Moreover, depth-dependent quenching analyses showed that Trp30 resides only 0.85 nm above the center of the lipid bilayer (Phillips et al. 2005). Given these findings, one might be concerned with the soft nature of the membrane; specifically, it is not clear as yet whether only the hydrophobic patch of HaTx1 protrudes into the hydrophobic core of the membrane (as has conventionally been thought) or whether the entire HaTx molecule dimples into the membrane and resides at a deep position possibly accompanied by meniscus formation. Here, we perform simulation analyses of HaTx1 in lipid bilayer membranes. The potential effect of the attractive force on HaTx1 from the opposite (inner) leaflet-lipid head groups and its effect on the membrane structure and the equilibrium positioning of HaTx1 are evaluated. Molecular dynamics simulation studies of HaTx1 may provide insights into the relative importance of the flexibility of the head group layers as well as at least two types of peptide–lipid interactions: the local type (between the peptide and the *cis*-side membrane leaflet) and the long-range type (between the peptide and the opposite leaflet). The importance of non-cutoff-type methods accounting for long-range electrostatic forces is also discussed.

Experimental procedure

In this study, we use the term "bilayer center" to indicate the plane that is parallel to the membrane and contains the center of mass of the membrane. We let "com" indicate the "center of mass". We set the "*z*-axis" to be parallel to the membrane normal. The "*z*-distance" indicates the difference in the *z*-coordinates between two positions.

Systems

The Gromacs 3.2.1 program (Lindahl et al. 2001; Berendsen et al. 1995) was used with the united-atom force field ffgmx (http://www.gromacs.org). For DPPC (dipalmitoyl-phosphatidylcholine), the parameters modified by Tieleman and Berendsen (1996) were used. For HaTx1, we also tried GROMOS96 43a1 parameter set (van Gunsteren et al. 1996) and found that the choice between ffgmx and GROMOS96 did not affect the overall feature of the results. For water, the SPC model (Berendsen et al. 1987) was used. The bond lengths were constrained using the LINCS (Hess et al. 1997). The cutoff for Lennard-Jones interactions was set at 9 Å. To account for long-range electrostatic interactions, the Particle-Mesh Ewald (PME) algorithm (Darden et al. 1993; Sagui and Darden 1999) was used with the real-space cutoff at 9 Å and the maximal grid size of 0.12 Å. The integration time-step was set at 2 fs. The temperature was set at 310 K with Berendsen coupling (Berendsen et al. 1984). The pressure was controlled by the Berendsen barostat at 1 atm with the independent (semi-isotropic) coupling in the *xy*- and *z*-directions.

From the bilayer equilibrated by a 10 ns run starting with the coordinates available from Tieleman's group (http://www.moose.bio.ucalgary.ca/Downloads), a set of DPPC bilayers, namely 58/64 (number of DPPC of the upper/lower leaflets), was prepared by removing a cluster of an appropriate number of DPPC molecules. The coordinates for HaTx1 [1D1H by Takahashi et al. (2000)] were obtained from the Brookhaven Protein Databank. To embed HaTx1 into the membrane, SwissPDBviewer (http://www.expasy.org/spdbv) was used to remove the molecular overlap. To keep the systematic bias minimal, only the minimally required horizontal movements of DPPC molecules away from the toxin were allowed. The distance between any atom of DPPC and those of HaTx1 was set at no less than 2 Å. The system was hydrated with 3,600 water molecules containing 10 sodium and 12 chloride ions.

Unless otherwise noted, equilibration runs were carried out for 1 ns constraining the HaTx1 atoms, followed by 5–7 ns free production runs. In one set of analyses, to prevent the membrane deformation, the *z*-distance between the com of HaTx1 and that of the 10 DPPC molecules belonging to the lower leaflet of the membrane was fixed. Analysis of the properties of the system and movement of the toxin was done using a combination of Gromacs utilities and our own analysis programs.

Calculations were carried out on 40 desktop PCs with Intel 2.8 GHz processors with or without parallelization. Simulation time on one PC was ~35 h/ns. All molecular images in this report were made with VMD (Humphery et al. 1996).

RMSD

To ensure the validity of a simulation, the conformational stability of HaTx1 during a run was assessed by measurement of the conformational drift, as given by the Cα atom mean-square deviation (RMSD), from the initial structure. When ten randomly chosen trajectories in Fig. 2a were examined, the RMSD for the middle segment (from G8 to W30) was small, ranging from 0.03

to 0.20, showing a high degree of stability in this segment. Thus, the middle segment is stable and assumes a structure similar to that found using NMR, most likely due to the presence of three disulfide bonds (Takahashi et al. 2000). On the other hand, both terminal segments exhibited a relatively large RMSD: for the N terminus, E1 0.46; C2, 0.40; R3, 0.21; Y4, 0.35; L5, 0.39; F6, 0.44; G7, 0.44 and C terminus, D31, 1.04; F32, 1.53; T33, 1.94; F34, 1.95; S35, 1.66. However, conformational drift of both terminals was small after simulation lasted for a sufficient time. A typical RMSD calculated for a 5 ns period following the initial 5 ns, with respect to the structure at the beginning of the period, was <0.11 for all residues. Therefore, the N- and C-terminal ends are also stable, but assume a conformation distinct from the NMR-determined structure. Detailed inspection suggested that the conformations of both terminals are largely determined by the interactions between the terminals and the DPPC molecules (unpublished data). Thus, during the simulation trajectories, the structural integrity of HaTx1 was largely maintained and the conformational variation of HaTx1 was reasonably small.

Azimuthal orientation

The orientation of HaTx1 is indicated by (θ_1, θ_2), where θ_1 is the angle of v_1 (the vector from Cα of Asp14 to that of Thr11) and θ_2 is the angle of v_2 (the vector from Cα of Asp14 to that of Gly20) with respect to the plane perpendicular to the z-axis.

Results

We first performed a set of simulations without introducing any constraint on atomic positions or on inter-atomic distances, except for fixed bond length. The initial HaTx1 orientation was chosen such that the hydrophobic protrusion of HaTx1 is at the bottom, as suggested by Lee et al. (2003) (Fig. 1). This orientation is represented by (30, −10) using the θ_1, θ_2 angles as explained in Experimental procedure. We chose three different depths in the membrane as the initial positions of HaTx1 (Fig. 2a). Based on RMSD analysis, we concluded that the overall structure of HaTx1 was maintained during the simulations (see Experimental procedure).

With the com (center of mass) of HaTx1 initially at 0.8 nm above the bilayer center, HaTx1 moved a small distance in the z-direction. Supplementary Material S1 shows a typical result, in which the distance between the com of HaTx1 and that of the membrane changed from 0.9 nm (at the initial frame) to 0.8 nm at 6 ns but showed a very small change after the initial 6 ns. In contrast, when the com was 0.3 nm above the bilayer center, HaTx1 moved outward, whereas when the com was 1.3 nm above the bilayer center, HaTx1 moved downward (inward) to a deeper position (Fig. 2a). Additional simulations showed that this trend in inward movement was weak when HaTx1 was placed 1.5 nm above the bilayer center (unpublished data). In addition, the trajectories with HaTx1 in a deep position (com 0.7–0.8 nm above the bilayer center) exhibited lower levels of potential energy than those trajectories with HaTx1 located in a shallow position (Fig. 2a), although in general such potential energy data should be carefully interpreted because of large variances.

Typically, ~20 (and ~35, respectively) water molecules were present in the space between HaTx and the hydrophobic core of the membrane when HaTx1 was 1.5 nm (and 0.7 nm, respectively) above the bilayer center (S2 of Supplementary Material, and data not shown). On the other hand, the average number of hydrogen bonds (based on the default criteria of Gromacs) formed between HaTx1 and DPPC was 12.3 when the HaTx1 com was located at 1.5 nm from the bilayer center in the Gromacs analyses. This suggests a mechanism for the stabilization of HaTx1 at the depth of 1.5 nm above the bilayer center.

A local deformation (thinning) of the membrane in close proximity to HaTx1 was observed when the HaTx1 com was 0.5–0.9 nm above the bilayer center ('x1.0' of Fig. 3). Figure 3 shows the average distance between the

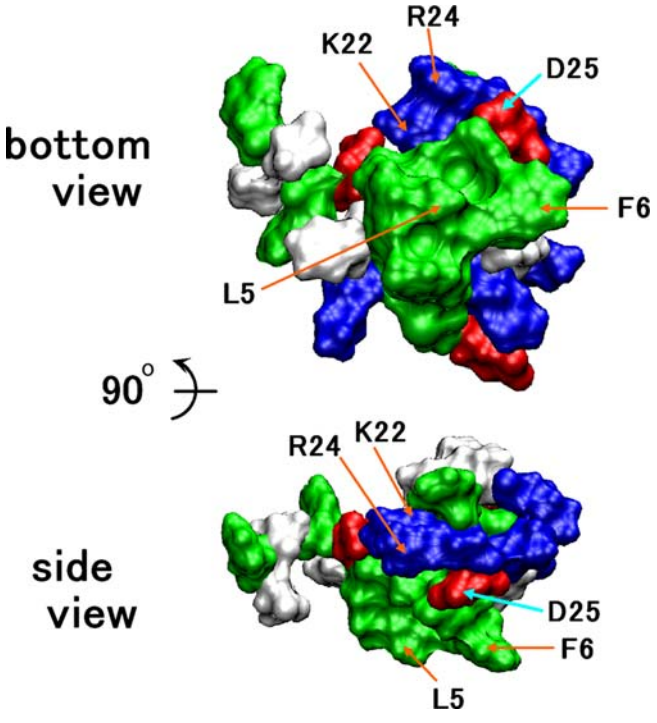

Fig. 1 Initial orientation of HaTx1. The bottom and side views of the initial orientation used for simulations. This orientation is represented as (θ_1, θ_2) = (30, −10) using the angles as explained in the Experimental procedure. The hydrophobic patch is oriented around the center of the normal view and at the bottom of the side view as in the Takahashi et al. (2000). Hydrophobic residues (Ala, Cys, Ile, Leu, Met, Phe, Pro, Trp, Tyr and Val) are *green*; basic (Arg and Lys) are *blue* and acidic (Asp and Glu) residues are *red*

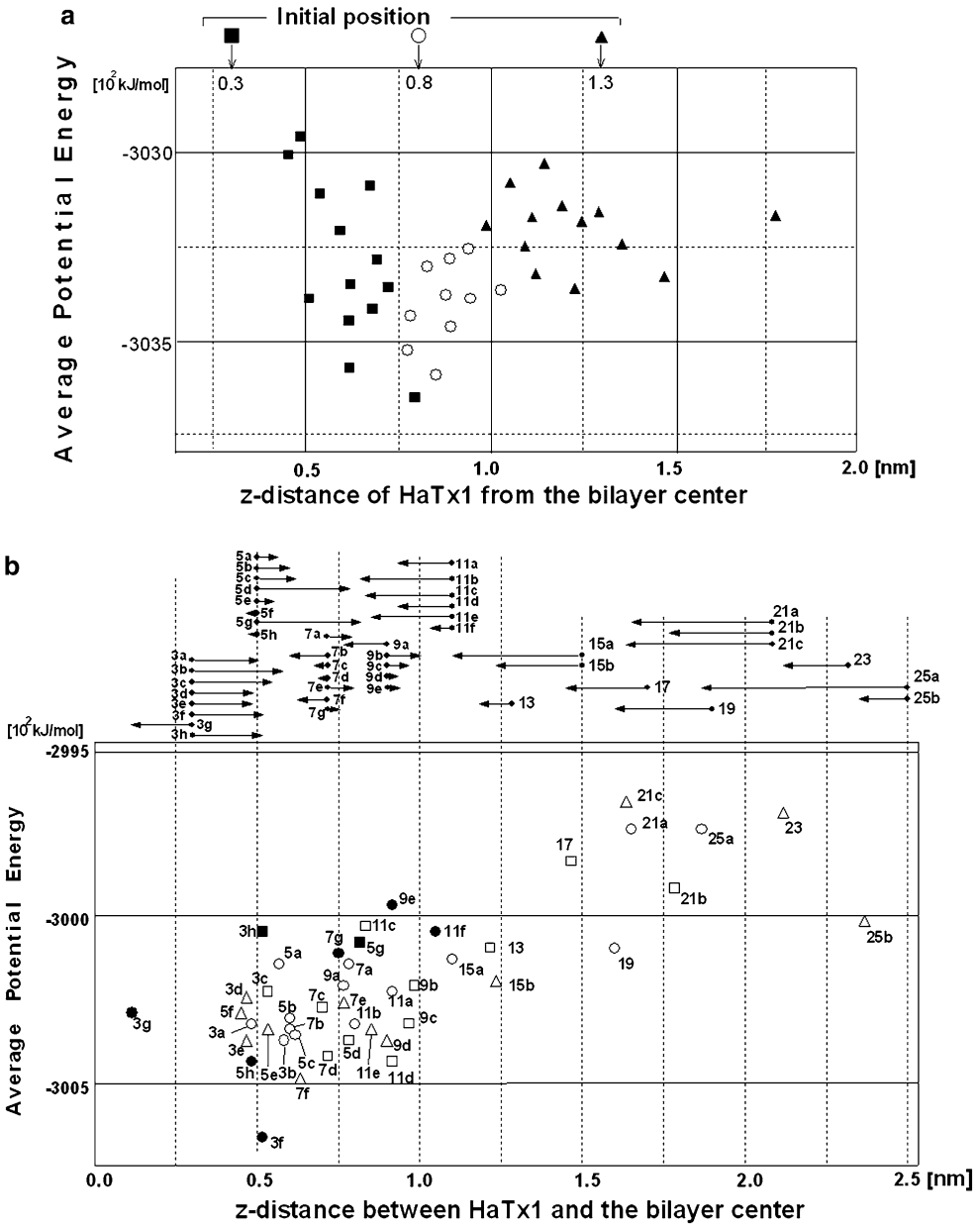

Fig. 2 The potential energy of the system and the HaTx1 position at the end of simulations. **a** Results for the free simulations. The total potential energy averaged over the last 500 ps is indicated by the altitude, whereas the *abscissa* represents the final *z*-distance between the com of HaTx1 and that of all DPPC molecules. **b** The results for simulations in which the lower membrane leaflet was constrained. Each plot is labeled to reflect the initial *z*-distance; e.g., "9a" indicates that the HaTx1 com was initially located at 0.9 nm above the bilayer center. The initial and final *z*-positions of the HaTx1 com for each simulation are also depicted using an *arrow* shown at the *top* of the graph. *Different symbols* indicate the orientations of HaTx1 at the beginning of the trajectories; (θ_1, θ_2) for each symbol is: *open circles* (−36.3, 9.3); *open squares* (−6.1, 13.5); *open triangles* (−18.4, 2.1); *filled circles* (6.4, 24.4); *filled squares* (4.5, 84.8)

outer and inner leaflets based on the procedure given in the legend. This local deformation (thinning) was achieved by the upward (outward) movement of approximately 10 DPPC molecules located in the lower (inner) bilayer leaflet underneath HaTx1 and by the inward movement of the DPPC head groups of nearby DPPC in the outer leaflet (S2 of Supplementary Material). There was less membrane thinning when HaTx1 was positioned near or above the outer membrane/water interface (~1.5 nm) (data not shown).

Therefore, when HaTx1 was in a shallow position (~1.5 nm), our system largely reproduced the shallow binding model suggested by Lee et al. (2003), but when HaTx1 was in a deeper position (< 1.3 nm), the system was unstable leading to membrane deformation (thinning) and the inward movement of HaTx1. Further analyses, where the atomic charges were varied, showed that the electrostatic force between the negatively charged head groups of the inner (opposite) leaflet lipids and the positively charged residues of HaTx1 is the primary source of the attractive force (see Discussion).

HaTx1 movement in the membrane with constraints on the inner leaflet

Although the membrane deformation was significant and reproducibly found, the upward movement of the inner leaflet lipids is not straightforward to test experimentally. Therefore, rather than focus on the membrane deformation, we focused on the *force* acting on HaTx1 under various conditions. We can either allow or suppress the membrane deformation by introducing constraints on the vertical movements of the inner leaflet of

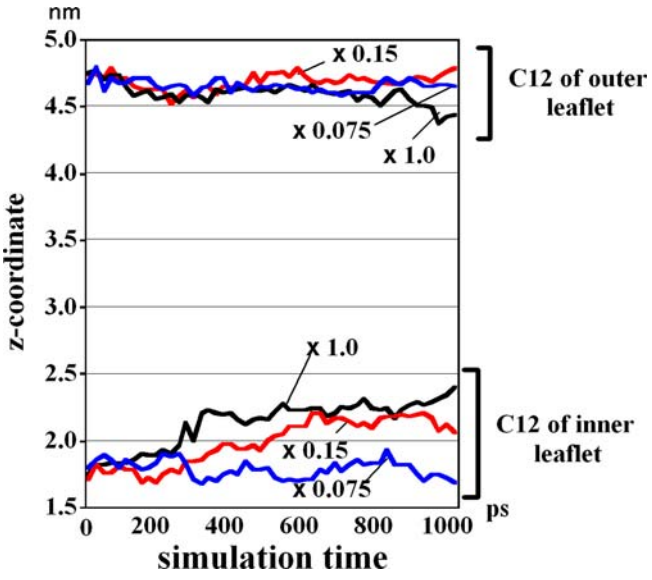

Fig. 3 Time course of the *z*-coordinates of C_{12} of outer- and inner leaflet DPPC near HaTx1. (C_{12} is the carbon atom forming an *o*-ester with the *sn*-2 acyl chain.) Shown are the average *z*-coordinates of C_{12} of these 12 DPPC molecules surrounding and the 12 molecules underneath HaTx1, respectively. "x0.15" and "x0.075" indicate the degrees of downscaling of atomic charges relative to "x1.0", the original charge set. Changes over representative deep binding mode trajectories are shown

the DPPC molecules in order to study the force separately from the gross membrane deformation. In practice, we ran another set of simulations in which the *z*-coordinate of the com of the 12 DPPC molecules located under HaTx1 was harmonically constrained. Under these conditions, the upward movement of the inner leaflet was not observed, but importantly, the meniscus formation (dimpling) of the outer leaflet still occurred. Figure 4a, b shows snapshots at 5 ns where the HaTx1 com is 0.7 nm above the bilayer center. As expected, such meniscus formation was not observed when HaTx1 was at a depth of 1.5 nm above the bilayer center (Fig. 4c). As the arrows in Fig. 2b show, when the HaTx1 com was initially positioned >1.1 nm above the bilayer center, HaTx1 moved to a deeper position in the membrane. When the HaTx1 com was <0.5 nm above the bilayer center, HaTx1 moved outward (Fig. 2b). When the HaTx1 com was ~0.7–0.8 nm above the bilayer center, the net HaTx1 movement was small. Therefore, even when the vertical movement of the group of DPPC molecules of the inner membrane leaflet was constrained, the preferred position of HaTx1 was ~0.7–0.8 nm above the bilayer center. This is a deeper position than the lipid/water interface (~1.5 nm if there is no deformation). The occurrence of dimpling implies that the energetic cost for meniscus formation in the outer leaflet is smaller than the energetic advantage obtained by the deep positioning of HaTx1.

Therefore, when HaTx1 was placed slightly below 1.5 nm above the bilayer center, HaTx1 spontaneously moved toward the interior of the membrane. Very long simulation runs (~20 ns) with HaTx1 (and each of the deprotonated variants of HaTx1) 1.5 nm above the bilayer center showed slow but reproducible inward movement of (wild-type) HaTx1 even at 1.5 nm from the bilayer center (data not shown).

With respect to the reorientation, inspection of many trajectories starting from various orientations showed that the previously suggested orientation $(\theta_1, \theta_2) = (30, -10)$ was largely stable when HaTx1 was located ~1.5 nm above the bilayer center (Supplementary Material S3). There was no clear "target" to which the orientation converged, although $(\theta_1, \theta_2) = (10, -10)$ appeared somewhat representative. On the other hand, when HaTx1 is located deep (~0.7 nm above the bilayer center) in the membrane, HaTx1 tends to assume an orientation close to $(-10, -20)$ (Supplementary Material S3), most likely because the region containing Arg24 and Lys26 experiences a stronger inward pull than the other regions (see Discussion).

Discussion

Collectively, the results shown above suggest that the surface-binding mode has limited stability and the meniscus formation appears to provide a favorable condition that allows HaTx1 to move inward.

The electron paramagnetic resonance (EPR) saturation method for the membrane immersion depth measurement (Hubbell and Altenbach 1994) is fascinating, but at least our simulations showed that the correct folding of HaTx1 critically depends on the six cysteine residues and therefore the utilization of the cysteine-less mutant for spin labeling may be impractical (data not shown). The NMR method can provide information about the local environments around the specific atoms and the order parameter of lipids, but it is not clear whether specific models can be derived when the membrane deformation is possible and several water molecules could also be drawn into the concave created by the deformation.

It has recently been shown that bromine atoms near the middle of the hydrocarbon tail (C9, C10) are more effective at quenching the fluorescence by Trp30 than bromine atoms at (C6, C7) (where "C1" is the carbon bonded to the carbonyl oxygen) (see Fig. 4 of Phillips et al. 2005). Bromine atoms at (C11, C12) are slightly less effective than those at (C9, C10), but more effective than (C6, C7). Moreover, depth-dependent quenching analyses show that Trp30 resides 0.85 nm above the center of the lipid bilayer.

What type of binding mode (surface or deep) is consistent with these quenching results? While the authors suggested a surface-binding mode, we would like to re-examine this idea because neither the possibility of meniscus formation nor the reorientation of HaTx1 was considered by Phillips et al. (2005). Our analyses show that the fluorescent-quenching results fit well to the deep binding mode. In fact, in our

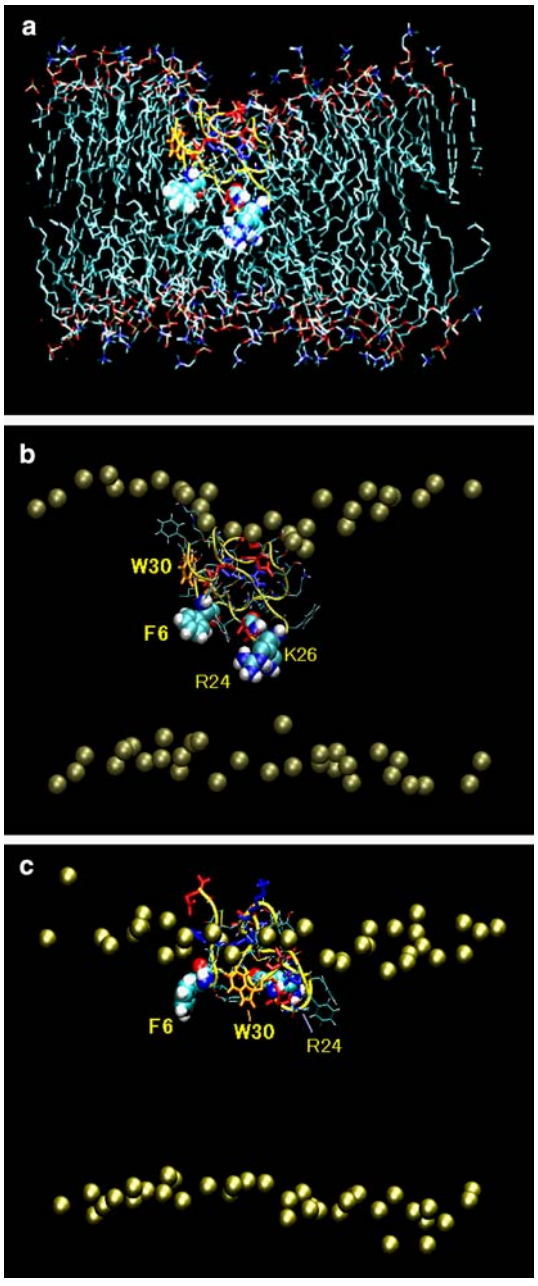

Fig. 4 Snapshots taken from representative trajectories. Shown are the results for the analyses with the constraints on the inner leaflet. **a** A snapshot at 5 ns of the Gromacs simulation with the HaTx1 com initially located 0.7 nm above the bilayer center. For clarity, only the non-water atoms contained in a slice of 3 nm thickness is shown. HaTx1 can be viewed more clearly in **b**. The peptide backbone is shown by an *yellow tube*. **b** The same as in **a** but a different representation. The phosphorus atoms of DPPC are shown by *ocher spheres*. DPPC acyl chains are not shown. The sidechain of Arg24 is shown by *blue spheres*. Phe6 is shown by *light blue* and *white spheres*. The charged residues other than Arg24 and Lys26 are shown as a *blue* (Arg, Lys) or *red* (Asp, Glu) *licorice*. **c** A snapshot at 5 ns of the Gromacs simulation, with the HaTx1 com initially located 1.5 nm above the bilayer center

simulations, only when the HaTx1 com was 0.7 nm above the bilayer center (deep mode) was Trp30 located near ~C8, which is reasonably consistent with the fluorescent-quenching results. (Representative results are shown as the upper two figures of the Electronic Supplementary Material S4.) With HaTx1 ~1.5 nm above the bilayer center, Trp30 was located as high as C3 and the Trp30 position with respect to the membrane plane position was found ~1.3 nm above the bilayer center, which is inconsistent with 0.85 nm obtained by the quenching analyses (the bottom figure of Supplementary Material S4). It is interesting to note that for the positioning of HaTx1 near (C9, C10), the meniscus formation necessitates an even deeper positioning of HaTx1 than is considered for a "non-flexible" membrane. We believe that molecular dynamics simulation studies can be useful when spectroscopic data are interpreted taking into account the flexibility of polar head groups of the membrane.

Our findings suggest the presence of an attractive force between HaTx1 and DPPC of the inner leaflet of the membrane. HaTx has two arginine, four lysine, one glutamine and three aspartate residues and a net charge of $+2e$ under the default protonation state at pH 7.0 (Takahashi et al. 2000). The following results show that the attractive force is due to an electrostatic force created by negative charges of the head groups of the inner (opposite) leaflet lipids. When each atomic charge of the 12 DPPC molecules (residing beneath HaTx1) was downscaled by multiplying by 0.0–0.075, no appreciable outward movement of DPPC occurred (Fig. 3 and unpublished data). When downscaled by 0.15, the outward movement of the inner leaflet of DPPC occurred (Fig. 3). When we introduced a cutoff (instead of the PME method) eliminating the long-range (>0.8 nm) electrostatic force, no outward movement of DPPC was observed (unpublished data). This is of technical relevance in that the treatment of long-range electrostatic energy can influence the overall structure of a membrane embedded with a charged peptide.

Membrane thinning was also observed in simulations of two additional systems: (1) when we doubled the size of DPPC membrane and positioned one HaTx1 molecule on each side of the membrane (roughly with the 2_1 symmetry), and (2) when a POPC (palmitoyl-oleyl-phosphatidylcholine) membrane was used (unpublished data).

Of note, the 0.15-fold downscaling brings the atomic charges down to a value much smaller than in any force field currently accepted (e.g., a carbonyl oxygen, $-0.09e$; an ester oxygen, $-0.11e$; and a carbon of carboxyl group, $0.11e$). Therefore, an influential strength of force is likely to exist between HaTx1 and the inner leaflet of DPPC in physiological system as well. The small dielectric constant (ε) of the hydrophobic interior may allow for such a long-range electrostatic force (ε of palmitic acid ~2.3; water ~88.0).

When the com of HaTx1 was 0.7 nm above the bilayer center, HaTx1 generally reoriented toward (θ_1, θ_2) = ~(−10, −20) (Supplementary Material S3). In this orientation, the sidechains of Arg24 and Lys26 became as deep as the hydrophobic protrusion (i.e., Leu5 and

Phe6) (Fig. 4b, d). We also performed extensive analyses using "Pull-code" of Gromacs to measure the force on the Arg24 and Lys26 (i.e., we used the "constraint" method described in Marrink and Berendsen 1994 and used in Shepherd et al. 2003) and the results showed that the force was consistently inward and its strength was within the range of ~50–100 kJ/mol/nm, except for the case that the residues were ~1.0 nm above the bilayer center, when the force was negligibly weak (S5 of the Supplementary Material). It is thus likely that the long-range electrostatic interaction plays an important role in determining the position of HaTx1 within the membrane. However, it is also possible that the hydration of R24 and K26 by the water molecules entering from the inside surface of the membrane may also provide a favorable condition to the deep positioning of R24 and K26. It also seems possible that in the initial phase of the interaction of HaTx and the membrane, the chance for the formation of water pores in the proximity of HaTx may increase [for the transient water pores, see, e.g., Deamer and Bramhall (1986) and Leontiadou et al. (2004)]. We performed simulations similar to the one shown in Fig. 2b except for the deprotonated Arg24 and Lys26 (thus, the positive charge of 2*e* was removed). The results show a shallow positioning of Arg24 and Lys26 as well as a slight outward movement of the HaTx1 com, suggesting that the deep positioning of Arg24 and Lys26 for the wild-type HaTx1 is dependent on the positive charges of the residues (Fig. 5). Of note, the thinning of the bilayer and disordering of the lipid chains induced by an antifungal peptide MB21 have been reported in the molecular dynamics simulation study by Tieleman's group (Shepherd et al. 2003). The disorder of not only the *cis* but also the *trans* (i.e., opposite) monolayer of the bilayer interacting with an acyl-anchored peptide has been shown to occur in the simulation study by Jensen et al. (2004). Aliste et al. (2003) have also reported that the pentapeptides containing Arg or Lys can perturb the atom distribution of the lipids, making the distribution of groups near the carbonyl area narrower. Compared with these cases, the effect of HaTx1 on membrane structure appears to be more dependent on the long-range electrostatic interactions between HaTx1 and the lipids of the inner leaflet and/or on the hydration of the charged residues by the water molecules that penetrate into the membrane.

The electrostatic potential mapped on the surface of HaTx1 calculated under simplified condition [i.e., the use of partial (atomic) charges and the isotropic application of the dielectric coefficient] shows that HaTx1 has a biased surface-mapped potential (http://www.homepage3.nifty.com/~gene/charge.html). The wide region containing Lys22, Arg24 and Lys26 is generally rich in positive charges, whereas only the small region near the carboxy-terminal is negatively charged. The anisotropic distribution of the charges may contribute to the rotational instability of HaTx1.

Intriguingly, when we performed the simulations similar to the one shown in Figs. 2b and 4 but with the short peptide KFRDK (corresponding to the 22–26 of HaTx1) placed 1.2 nm above the bilayer center, an *outward* movement of the peptide was consistently observed and the peptide resided at the depth of the phosphorus and carbonyl oxygen atoms (~1.5 nm), despite of the same net charge as HaTx1 (+2*e*) (Fig. 6). Therefore, it appears that the behavior of the peptide within the membrane significantly depends not only on the total charge of the peptide but also on the volume and/or structure of the peptide. It is tempting to hypothesize that space occupation can lead to weakening of the local interactions relative to the long-range interactions. We are currently trying to obtain a clearer view on the effect of the size of the charged peptide on the balance of forces acting on the peptide.

The S4 segment of Kv channels (the voltage sensor) has been considered to be confined within a hydrated "canal" (or in a more recent model, a "crevice") and thus shielded from the hydrophobic environment of the membrane in the so-called canonical models (e.g., Laine et al. 2003). A recent version of a canonical model suggests a rotational (and outward) movement, rather than an upward translocation, of the S3–S4 segment upon depolarization (Chanda et al. 2005), which is in agreement with the finding of small vertical movement of the *Shaker* K^+ channel voltage sensor upon depolarization (Posson et al. 2005). In the paddle model, on

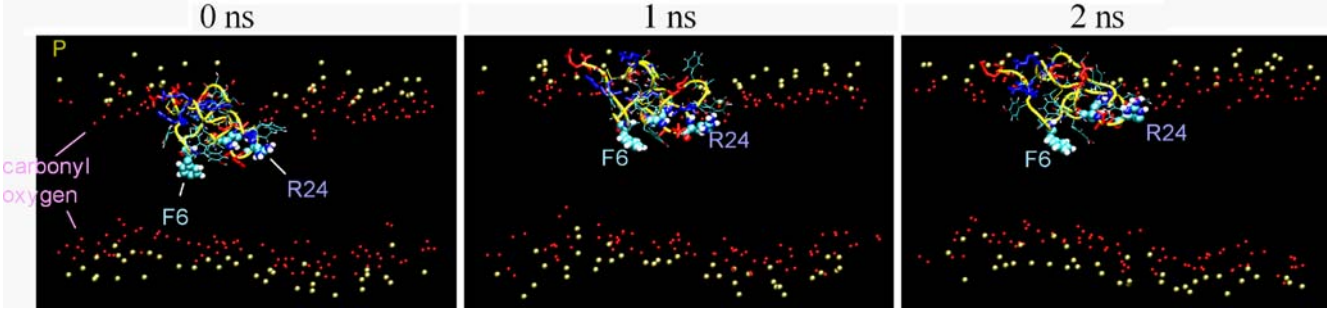

Fig. 5 Snapshots from the simulations in which both Arg24 and Lys26 are deprotonated. Representation method is similar to Fig. 4 except for the carbonyl oxygen atoms shown by *small red spheres*. The initial position of the HaTx1 com was 1.2 nm above the bilayer center. Note that no inward movement of HaTx1 or Arg24/Lys26 was observed

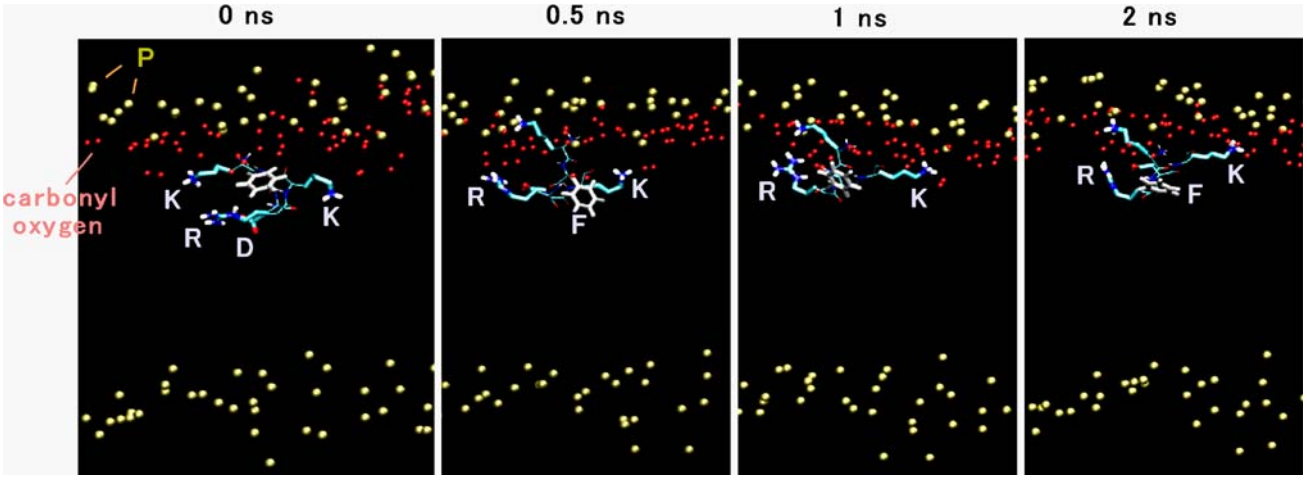

Fig. 6 Snapshots from the trajectory of the simulation containing the peptide KFRDK corresponding to the segment 22–26 of HaTx. The com of the peptide was initially set at 1.2 nm above the bilayer center. In contrast to the results with HaTx1 (e.g., Fig. 4), the peptide moved outward to the depth of the polar head groups of the outer leaflet DPPC

the other hand, a paddle-like structure formed by S4 and the C-terminal half of S3 has been thought to carry the charged segment across the bilayer with >20 Å movements entirely through the lipid based on the study with the avidin–biotin technique (Jiang et al. 2003). Although this large movement has not been supported by other experiments, the analyses using EPR supported the view of the peripheral positioning of S4, arguing against the models predicting a crevice shielding the S4 segment (Cuello et al. 2004). In general, little is known about the position of the voltage sensor in the closed state of the channels.

Our results suggest that HaTx1 prefers a deep positioning and we estimate that the associated free energy for the deep binding relative to the shallow binding is not far from ~100 kJ/mol (Supplementary Material S5 and data not shown). Given that the gating charge per channel subunit is 3.25e (Hille 2001) and assuming it experiences a decrease of −100 mV on depolarization, the energy reduction upon the translocation should be approximately ~30 kJ/mol, which is easily counteracted by the deep positioning of HaTx1, suggesting that the deep positioning of HaTx1 can suppress the outward movement of the voltage sensor. One may point out that our model brings the hydrophobic patch of HaTx, which is likely to contact with the voltage sensor (Wang et al. 2004), close to the position of the paddle as depicted in the study by Jiang et al. (2003). At least, our findings seem to be consistent with the view that the S3–S4 segment has a substantial flexibility (Sands et al. 2005), but less consistent with the view that HaTx, while located at a shallow position, binds to S4 confined within a crevice in the closed state (Phillips et al. 2005). The deep positioning of HaTx also appears to be consistent with its loss of affinity to the voltage sensor after stimulation by a depolarizing pulse (Swartz and MacKinnon 1995; Phillips et al. 2005). We surmise that, as the voltage sensors carry the bound HaTx outward as a cargo upon activation (Fig. 2d of Phillips et al. 2005), this outward translocation of HaTx may increase the force pulling the HaTx inward (back to the inner leaflet) helping to unbind the HaTx from the voltage sensors. Another unusual characteristic of HaTx is its very slow action ($\tau = 114$ s) despite the high affinity to the voltage sensor of Kv2.1 channel ($K_d = 42$ nM) (Swartz and MacKinnon 1995). This phenomenon suggests that the equilibrium position of HaTx is different from that of the binding site on the voltage sensor and therefore could be better explained by the deep positioning of HaTx than by the shallow binding mode, if the HaTx-binding site of the voltage sensor (see, e.g., Lee et al. 2003) is located at a shallow position as shown in Chanda et al. (2005). Therefore, while the paddle model may have to be revised in the light of the recent experimental findings and, specifically, while the paddle in the closed state may be at a higher position than the position previously proposed by Jiang et al. (2003), the paddle model seems to provide a simple view explaining our results as well as the loss of affinity of HaTx to the voltage sensor after stimulation (Phillips et al. 2005). More spectroscopic and theoretical efforts have to be done in order to elucidate how HaTx interacts with the voltage sensors of voltage-dependent channels.

Finally, although it is currently difficult to determine accurately the equilibrium position of a peptide within the membrane, molecular dynamics simulation allows us to examine the balance of a variety of forces on a peptide and their impact on the overall structure of the membrane. This can be useful for interpreting spectroscopic data on peptide positioning in membranes, especially when there is an ambiguity due to the effect of meniscus formation by the polar head groups of the membrane.

Acknowledgements We thank the anonymous reviewers for their helpful suggestions. This work was supported by Grant-in-Aid for Scientific Research from the Ministry of Education, Culture, Sports, Science, and Technology of Japan.

References

Aliste MP, MacCallum JL, Tieleman DP (2003) Molecular dynamics simulations of pentapeptides at interfaces: salt bridge and cation-π interactions. Biochemistry 42:8976–8987

Ash WL, Zlomislic MR, Oloo EO, Tieleman DP (2004) Computer simulations of membrane proteins. Biochem Biophys Acta 1666:158–189

Berendsen HJC, Postma JPM, van Gunsteren WF, DiNola A, Haak JR (1984) Molecular dynamics with coupling to an external bath. J Chem Phys 81:3684–3690

Berendsen HJC, Grigera JR, Straatsma TP (1987) The missing term in effective pair potentials. J Phys Chem 91:6269–6271

Berendsen HJC, van der Spoel D, van Drunen R (1995) GROMACS: a message-passing parallel molecular dynamics implementation. Comput Phys Commun 91:43–56

Chanda B, Asamoah OK, Blunck R, Roux B, Bezanilla F (2005) Gating charge displacement in voltage-gated ion channels involves limited transmembrane movement. Nature 436:852–856

Cuello LG, Cortes DM, Perozo E (2004) Molecular architecture of the KvAP voltage-dependent K^+ channel in a lipid bilayer. Science 306:491–495

Darden T, York D, Pedersen L (1993) Particle Mesh Ewald: an *N*log(*N*) method for Ewald sums in large systems. J Chem Phys 98:10089–10092

Deamer DW, Bramhall J (1986) Permeability of lipid bilayers to water and ionic solutes. Chem Phys Lipids 40:167–188

Domene C, Bond PJ, Sansom MS (2003) Membrane protein simulation: ion channels and bacterial outer membrane proteins. Adv Prot Chem 66:159–193

Forrest LR, Sansom MS (2000) Membrane simulations: bigger and better? Curr Opin Struct Biol 10:174–181

van Gunsteren WF, Kruger P, Billester SR, Mark AE, Eising AA, Scott WRP, Huneberg PH, Tironi IG (1996) Biomolecular simulation: the GROMOS96 Manual and User Guide. BIOMOS/Hochschuleverlag AG and der ETH, Zürich

Hansson T, Oostenbrink C, van Gunsteren WF (2002) Molecular dynamics simulations. Curr Opin Struct Biol 12:190–196

Hess B, Bekker H, Berendsen HJC, Fraaije JGEM. (1997) LINCS: a linear constraint solver for molecular simulations. J Comput Chem 18:1463–1472

Hille B. (2001) Ion Channels of Excitable Membranes, 3rd edn. Sinauer, Sunderland, pp 131–160, 611–614

Hubbell WL, Altenbach C (1994) Site-directed spin labeling of membrane proteins. In: White S (ed) Membrane Protein Structure: Experimental Approaches. Oxford University Press, New York, pp 224–248

Humphery W, Dalke A, Schulten K (1996) VMD—visual molecular dynamics. J Mol Graph 14:33–38

Jensen MO, Mouritsen OG, Peters GH (2004) Simulations of a membrane-anchored peptide: structure, dynamics, and influence on bilayer properties. Biophys J 86:3556–3575

Jiang Y, Ruta V, Chen J, Lee A, MacKinnon R (2003) The principle of gating charge movement in a voltage-dependent K+ channel. Nature 423:42–48

Laine M, Lin M-cA, Bannister JPA, Silverman WR, Mock AF, Roux B, Papazian DM (2003) Atomic proximity between S4 segment and pore domain in *Shaker* potassium channels. Neuron 39:467–481

Lee HC, Wang JM, Swartz KJ (2003) Interaction between extracellular hanatoxin and the resting conformation of the voltage-sensor paddle in Kv channels. Neuron 40:527–536

Leontiadou H, Mark AE, Marrink SJ (2004) Molecular dynamics simulations of hydrophilic pores in lipid bilayers. Biophys J 86:2156–2164

Lindahl E, Hess B, van der Spoel D (2001) GROMACS 3.0: a package for molecular simulation and trajectory analysis. J Mol Mod 7:306–317

Li-Smerin Y, Swartz KJ (1998) Gating modifier toxins reveal a conserved structural motif in voltage-gated Ca2+ and K+ channels. Proc Natl Acad Sci USA 95:8585–8589

Marrink S-J, Berendsen HJC (1994) Simulation of water transport through a lipid membrane. J Phys Chem 98:4155–4168

Phillips LR, Milescu M, Li-Smerin Y, Mindell JA, Kim JI, Swartz KJ (2005) Voltage-sensor activation with a tarantula toxin as cargo. Nature 436:857–860

Posson DJ, Ge P, Miller C, Bezanilla F, Selvin PR (2005) Small vertical movement of a K+ channel voltage sensor measured with luminescence energy transfer. Nature 436:848–851

Ruta V, Jiang Y, Lee A, Chen J, MacKinnon R (2003) Functional analysis of an archaebacterial voltage-dependent K+ channel. Nature 422:180–185

Sagui C, Darden TA (1999) Molecular dynamics simulations of biomolecules: long-range electrostatics effects. Annu Rev Biophys Biomol Struct 28:155–179

Sands ZA, Grottesi A, Sansom MS (2005) The intrinsic flexibility of the Kv voltage sensor and its implications for channel gating. Biophys J (in press)

Shepherd CM, Vogel HJ, Tieleman DP (2003) Interactions of the designed antimicrobial peptide MB21 and truncated dermaseptin S3 with lipid bilayers: molecular-dynamics simulations. Biochem J 370:233–243

Swartz KJ, MacKinnon R (1995) An inhibitor of the Kv2.1 potassium channel isolated from the venom of a Chilean tarantula. Neuron 15:941–949

Swartz KJ, MacKinnon R (1997) Hanatoxin modifies the gating of a voltage-dependent K+ channel through multiple binding sites. Neuron 18:665–673

Takahashi H, Kim JI, Min HJ, Sato K, Swartz KJ, Shimada I (2000) Solution structure of hanatoxin1, a gating modifier of voltage-dependent K(+) channels: common surface features of gating modifier toxins. J Mol Biol 297:771–780

Tieleman DP, Berendsen HJC (1996) Molecular dynamics simulations of fully hydrated DPPC with different macroscopic boundary conditions and parameters. J Chem Phys 105:4871–4880

Tieleman DP, Marrink SJ, Berendsen HJC (1997) A computer perspective of membranes: molecular dynamics studies of lipid bilayer systems. Biochem Biophys Acta 1331:235–270

Wang JM, Roh SH, Kim S, Lee CW, Kim JJ, Swartz KJ (2004) Molecular surface of tarantula toxins interacting with voltage sensors in Kv channels. J Gen Physiol 123:455–467